 FDMP, vol.7, no.2, pp.201-216, 2011

Impact of the Vibrations on Soret Separation in Binary and Ternary Mixtures

S. Srinivasan[1] **and M. Z. Saghir**[1]

Abstract: CFD simulations have been made to understand the impact of the vibrations of the ISS on the thermodiffusion process. Simulations were made for two ternary hydrocarbon mixtures and one binary associated mixture. While one of the ternary mixture was at a pressure of 35 MPa, the second ternary mixture as well as the binary mixture were at a pressure of 0.101325 MPa. The analysis of the results showed that imposing the ISS vibrations had a profound effect on the *Soret effect* in all three systems. More precisely, in all three mixtures, a single convective flow cell is established. Such a cell is responsible for a mixing effect, destroying most of the *Soret* separation. Further, the vibrations have a more damaging effect on the low pressure systems than the high pressure mixture. This is because, at a lower pressure the fluids respond more easily to the applied vibrations.

Keywords: Soret effect, thermodiffusion, vibrations, CFD simulations.

1 Introduction

In the presence of a thermal gradient, constituents in a mixture tend to segregate into opposite directions. Some collect on the hot side and the others migrate towards the cold side. This phenomenon is called the *Soret effect* or *thermodiffusion*. Invariably, the establishment of this concentration gradient is constantly opposed by the molecular diffusion process which tends to reestablish the initial state of a uniform mixture. At steady state, when there is no mass flux, there is a net separation of the constituents. The Soret coefficient, S_T, is an indicator of this separation strength and is given by $S_T = D_T/D$, where D_T is the thermodiffusion coefficient and D is the molecular diffusion coefficient.

Investigation of purely diffusive processes is challenging since conducting investigations on earth is often marred by buoyancy induced convection. This challenge is mitigated by pursuing the experiments in the space platforms like the International

[1] Department of Mechanical and Industrial Engineering, Ryerson University, Toronto, Canada.

Space Station (ISS) and free flying satellites such as FOTON M3 (Van Vaerenbergh, Srinivasan, and Saghir, 2009; Srinivasan, Eslamian, and Saghir, 2009; Srinivasan and Saghir, 2009; Srinivasan, Dejmeck, and Saghir, 2010). However, experiments onboard ISS experience vibrations due to crew activities, onboard devices etc. These induce disturbances in the fluid being investigated for pure diffusion. There are several investigations on the microgravity environment and its impact on the fluid. Specifically, investigations have been made on the effect of the reduced gravity environment on the instability of the fluid (Merkin, 1967; Davidson, 1973; Gershuni and Zhukhovitsky, 1981; Gershuni, Kolesnikov, Legros, and Myznikova, 1999), thermophysical properties of the fluid mixtures (Monti, Savino, and Lappa, 2001; Savino and Lappa, 2003) as well as the *Soret* separation (Yan, Jules, and Saghir, 2007; Yan, Pan, Jules, and Saghir, 2007).

With respect to thermodiffusion in the reduced gravity environment, studies by Yan et al. (Yan, Jules, and Saghir, 2007; Yan, Pan, Jules, and Saghir, 2007) have shown that large static gravity can induce strong convective behavior in the fluid and thereby minimize the Soret separation process. The authors also noted that the low frequencies have a larger negative impact on the thermodiffusion process. However, Chacha et al. (Chacha, Faruque, Saghir, and Legros, 2002; Chacha and Saghir, 2005) found that at certain orientations of the experimental apparatus, the impact of these vibrations can be minimized.

In this study, the environment provided by the ISS has been investigated. Specifically, the impact of the vibrations, recorded by the accelerometers onboard the ISS, on the thermodiffusion process in two ternary hydrocarbon mixtures, viz., *methane* (nC_1)/*n-butane* (nC_4)/*n-dodecane* (nC_{12}) and nC_{12}/isobutylbenzene (IBB) /tetralin (THN), and a binary mixture of *isopropanol*/*water* is investigated. It is expected that with a better understanding of the environment of the ISS and conducting the experiments appropriately to mitigate the negative influences, it is possible to obtain very accurate results for the thermodiffusion studies in a wide variety of mixtures.

2 Governing Equations

In the present investigation, Computational Fluid Dynamics (CFD) simulations have been made to study the thermodiffusion in two ternary hydrocarbon mixtures (T1 and T2) and a binary associating mixture (B1). The composition, simulation conditions as well as the geometry of each system is summarized in Table 1.

For mixture T1, the details in this table corresponds to a recent experiment on the free flying satellite, FOTON-M3 (Srinivasan and Saghir, 2009). Likewise, for the binary mixture, B1, the mixture composition, operating conditions as well as

Table 1: Computational details of the three mixtures.

	Ternary mixt. (T1)	**Ternary mixt. (T2)**	**Binary mixt. (B1)**
Mixt. components	$nC_1/nC_4/nC_{12}$	nC_{12}/IBB/THN	water/isoprop.
Mixt. concentration	0.2/0.5/0.3	0.3333/0.3333/0.3333	0.9/0.1
Mixt. pressure, p [MPa]	35	0.101325	0.101325
Mixt. temp., T [K]	333	318	295.5
Hot wall temp., T_h [K]	338	323	298
Cold wall temp., T_c [K]	328	313	293
Domain size, $L_x \times L_y$ [cm $\times$ cm]	4×0.6	1×1	1×1
Computational cells	60×9	15×15	15×15

Table 2: Thermophysical properties of the three mixtures.

	Ternary mixt. (T1)	**Ternary mixt. (T2)**	**Binary mixt. (B1)**
Dynamic visc. [kg/m.s]	2.521×10^{-4}	3.998×10^{-4}	1.036×10^{-3}
Density [kg/m^3]	625.62	780.53	993.36
Thermal conductivity [W/mK]	0.1054	0.1308	0.522
Specific heat capacity [J/kgK]	2399.0	1877.2	3991.0

the domain size correspond to a recently concluded experiment onboard the ISS. The ternary mixture, T2, is an ongoing experiment on the ISS. The thermophysical properties of all the mixtures is summarized in Table 2 and have been obtained from the National Institute of Standards and Technology database (NIST, 2007).

In all simulations, the thermal gradient was applied in the horizontal direction of a two-dimensional domain by maintaining the left wall at a temperature T_h and the right wall at the colder temperature, T_c. Also, in all simulations, a no slip boundary condition was applied. The entire setup is considered adiabatic with respect to the outer ambience. To understand the diffusion process of all the components in the cavity, a complete set of the governing equations was solved.

For a weakly compressible flow, where density variations are due to fluctuations in

local temperature and concentration, the continuity equation is represented as:

$$\frac{\partial \rho}{\partial t} + \frac{\partial \rho u}{\partial x} + \frac{\partial \rho v}{\partial y} = 0. \tag{1}$$

In the above equation, t is the time and u and v are the velocities in the x and y directions, respectively. ρ is the density of the mixture that is computed using the Peng-Robinson equation of state for the ternary systems (Srinivasan and Saghir, 2010) and using the Perturbed Chain Statistical Associating Fluid Theory for the binary system (Parsa, Srinivasan, and Saghir, 2010).

In addition to the mass conservation equation, for the ternary mixtures, two species conservation equations have been employed:

$$\begin{aligned}\left(\frac{\partial}{\partial t}(\rho c_1) + \frac{\partial}{\partial x}(\rho u c_1) + \frac{\partial}{\partial y}(\rho v c_1)\right) &= \frac{\partial}{\partial x}\left(\rho\left(D_{11}\frac{\partial c_1}{\partial x} + D_{12}\frac{\partial c_2}{\partial x} + D_{T,1}\frac{\partial T}{\partial x}\right)\right) \\ &\quad + \frac{\partial}{\partial y}\left(\rho\left(D_{11}\frac{\partial c_1}{\partial y} + D_{12}\frac{\partial c_2}{\partial y} + D_{T,1}\frac{\partial T}{\partial y}\right)\right) \end{aligned} \tag{2}$$

$$\begin{aligned}\left(\frac{\partial}{\partial t}(\rho c_2) + \frac{\partial}{\partial x}(\rho u c_2) + \frac{\partial}{\partial y}(\rho v c_2)\right) &= \frac{\partial}{\partial x}\left(\rho\left(D_{21}\frac{\partial c_1}{\partial x} + D_{22}\frac{\partial c_2}{\partial x} + D_{T,2}\frac{\partial T}{\partial x}\right)\right) \\ &\quad + \frac{\partial}{\partial y}\left(\rho\left(D_{21}\frac{\partial c_1}{\partial y} + D_{22}\frac{\partial c_2}{\partial y} + D_{T,2}\frac{\partial T}{\partial y}\right)\right). \end{aligned} \tag{3}$$

For the binary mixture of *water/isopropanol*, a single species equation is used and is given by

$$\begin{aligned}&\left(\frac{\partial}{\partial t}(\rho c_1) + \frac{\partial}{\partial x}(\rho u c_1) + \frac{\partial}{\partial y}(\rho v c_1)\right) = \\ &\qquad \frac{\partial}{\partial x}\left(\rho\left(D_{11}\frac{\partial c_1}{\partial x} + D_{T,1}\frac{\partial T}{\partial x}\right)\right) + \frac{\partial}{\partial y}\left(\rho\left(D_{11}\frac{\partial c_1}{\partial y} + D_{T,1}\frac{\partial T}{\partial y}\right)\right). \end{aligned} \tag{4}$$

In the above equations, c_i is the mole fraction of respective species and T is the temperature of the mixture at the location (x,y) at a particular time, t. D_{ii} and D_{ij} represent the main term and the cross term diffusion coefficients. $D_{T,i}$ is the thermodiffusion coefficient of the i^{th} species. Since these coefficients depend on the mixture concentration that is non-uniform when $t > 0$ s, and constantly changing throughout the domain, they have to be treated as variables in computational domain. Accordingly, the CFD code used in this study is equipped with models for computing these diffusion coefficients (Ghorayeb and Firoozabadi, 2000). The species conservation at every location in the domain is completed with $\sum_i c_i = 1$.

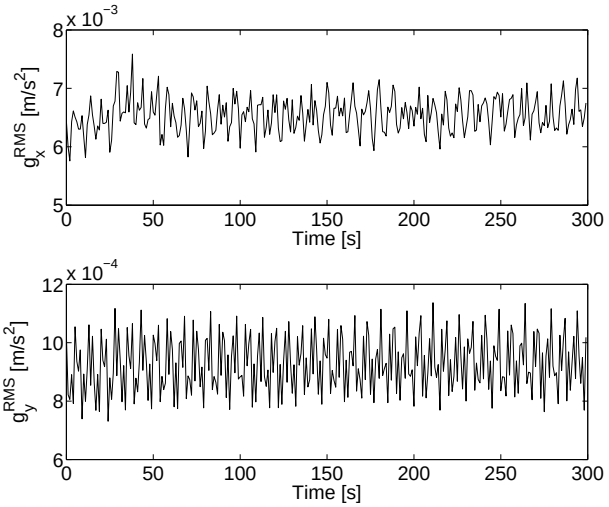

Figure 1: The demeaned RMS acceleration values in a 5 minute interval.

The x and y direction momentum conservation equations are:

$$\left(\frac{\partial}{\partial t}(\rho u)+\frac{\partial}{\partial x}(\rho uu)+\frac{\partial}{\partial y}(\rho vu)\right) = -\frac{\partial p}{\partial x}+\frac{\partial}{\partial x}\left(\mu\frac{\partial u}{\partial x}\right)+\frac{\partial}{\partial y}\left(\mu\frac{\partial u}{\partial y}\right)+\rho g_x, \quad (5)$$

$$\left(\frac{\partial}{\partial t}(\rho v)+\frac{\partial}{\partial x}(\rho uv)+\frac{\partial}{\partial y}(\rho vv)\right) = -\frac{\partial p}{\partial y}+\frac{\partial}{\partial x}\left(\mu\frac{\partial v}{\partial x}\right)+\frac{\partial}{\partial y}\left(\mu\frac{\partial v}{\partial y}\right)+\rho g_y. \quad (6)$$

In the above equations, p is the pressure in the domain. For the ternary hydrocarbon mixtures, the dynamic viscosity, μ, is calculated as a function of the composition of the mixture at a given location as per Lohrenz, Bray, and Clark (1964). For the binary mixture, a weighted average of the viscosities of the two pure components has been used to determine the dynamic viscosity at every grid point. In view of the fact that concentration of *isopropanol* is very small in this mixture, this approach is a reasonably good approximation of the mixture viscosity.

The source terms in the momentum equations account for the natural gravitational force as well as the accelerations that are imposed on the system due to the vibrations experienced by the space platform. In the present investigation, for each system, two cases have been considered. In the first case (*Ideal*), these source terms (g_x and g_y) have been set to zero. This corresponds to an ideal zero-gravity environment, i.e., a purely diffusive scenario. In the second case (*ISS*), the demeaned Root Mean Squared (RMS) values of the acceleration, as recorded by the on board accelerometer on the International Space Station, has been employed. More precisely,

for the *ISS* simulations, g_x and g_y have been given via the following equations

$$\begin{aligned} g_x &= g_x^{RMS}, \\ g_y &= g_y^{RMS}, \end{aligned} \tag{7}$$

where

$$\begin{aligned} g_i^{RMS} &= \sqrt{\frac{(g_i^{ISS}(1)-\bar{g}_i)^2+(g_i^{ISS}(2)-\bar{g}_i)^2+\cdots+(g_i^{ISS}(500)-\bar{g}_i)^2}{500}}, \\ \bar{g}_i &= \frac{\sum_{k=1}^{n} g_i^{ISS}(n)}{n}. \end{aligned} \tag{8}$$

In the above equations, g_i^{ISS} is the raw acceleration in the i-direction, recorded by the accelerometer onboard the ISS, $\bar{g}_i$ is the average acceleration in a one second interval and g_i^{RMS} is the RMS acceleration in each one second interval. Since the raw accelerations were recorded every 2 ms, five hundred samples were used to compute the RMS acceleration in each one second interval, i.e., $n = 500$. Typical RMS accelerations in a 5 minute interval that were applied in the simulations in this study are shown in Figure 1.

Finally, assuming a constant thermal conductivity and no internal energy generation, the energy equation that is used to compute the temperature distribution in the domain is given in terms of the fluid temperature, T, as:

$$c_p\left(\frac{\partial}{\partial t}(\rho T)+\frac{\partial}{\partial x}(\rho u T)+\frac{\partial}{\partial y}(\rho v T)\right)=k\left(\frac{\partial^2 T}{\partial x^2}+\frac{\partial^2 T}{\partial y^2}\right), \tag{9}$$

where c_p and k are the mixture's specific heat capacity and the thermal conductivity, respectively.

The governing equations along with the appropriate equation of state and boundary conditions have been solved for each cell in the two-dimensional cavity for the unknowns, viz., c_i, T, p, u, v, and ρ. For the computational meshes, a uniform resolution of 0.0667 cm in both directions was used for all three mixtures. This resolution has been validated in our recent work for two of the current mixtures, viz., Mixtures T1 and B1, respectively (Srinivasan, Dejmeck, and Saghir, 2010; Parsa, Srinivasan, and Saghir, 2010). A finite volume method is used for discretization of the governing equation. The discretized equations are solved using the Semi-Implicit Pressure Linked Equation (SIMPLE) algorithm as outlined by Patankar (1980).

All simulations have been made until about 18.5 hours to understand the impact of the vibrations on the flow behavior. This duration is longer than the experimental duration of the recently investigated binary mixture B1 on the ISS. Also, it is much

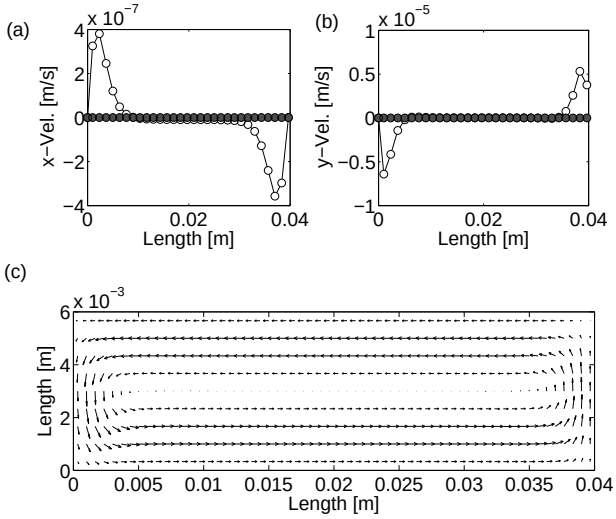

Figure 2: Velocities in the (a) x and (b) y directions along $y = 0.3$ cm line, and (c) the average flow profile in the last fifty seconds in the domain after about 18.5 hours. Open and closed symbols represent the *ISS* and *Ideal* case, respectively.

longer than the proposed experimental duration for mixture T2, that is underway on the ISS. For mixture T1, the diffusion time is about 56 hours (Srinivasan, Dejmeck, and Saghir, 2010). However, by about 18.5 hours a quasi steady state is reached and the concentration values at the hot and cold walls are within 0.04% of the steady state values (Srinivasan, Dejmeck, and Saghir, 2010).

3 Results & Discussions

3.1 Methane/n-butane/n-dodecane mixture

Figures 2a and 2b show the x and y direction velocities along $y = 0.3$ cm line after $t = 18.5$ hours, respectively, in the *Ideal* and the *ISS* cases. As seen in these figures, in the *Ideal* case (closed circle symbols) the flow velocities are very weak with velocity magnitudes of the order of 1×10^{-50} m/s. On the other hand, in the *ISS* case (open circle symbols) the velocities are higher with magnitudes of the order of 1×10^{-6} m/s. These higher velocities, that are primarily due to the imposed vibrations, result in a more structured flow with a well established flow cell in the domain (c.f. Figure 2c).

A general distribution of *methane*, *n-butane* and *n-dodecane* in the domain after

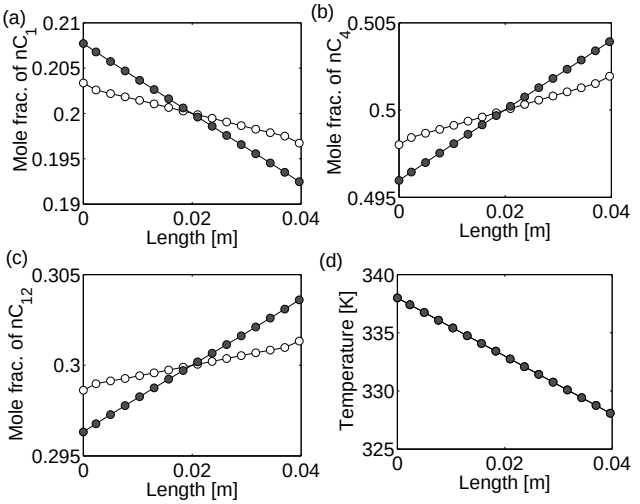

Figure 3: Distribution of (a) *methane* (b) *n-butane* (c) *n-dodecane* and (d) temperature along $y = 0.3$ cm line in the domain after about 18.5 hours. Open and closed symbols represent the *ISS* and *Ideal* case, respectively.

about 18.5 hours is shown in Figures 3a-3c, respectively. As seen in these figures, *methane* separates towards the hot side whereas *n-butane* and *n-dodecane* separate towards the cold side. This separation tendency is similar to the experimentally observed trend (Srinivasan and Saghir, 2009).

An interesting observation in these figures is that unlike the *Ideal* case, the separation is much weaker in the *ISS* case. This is a direct consequence of the vibrations that introduce a convective flow in the domain that destroys the *Soret* separation. From a closer look at these figures we can observe that the concentration values from the *ISS* and *Ideal* cases are in excellent agreement at $(x,y) = (2\text{ cm}, 0.3\text{ cm})$. However, the disagreement between these cases increases as we move towards the lateral walls. This is attributed to the velocity values that are very small at the center of the domain and increase as we move closer to the walls ($x = 0$ cm and $x = 4$ cm).

Similarly, the otherwise linear temperature profile in the *Ideal* case also experiences a very small variation due to the imposed vibrations. However, this is much subdued and cannot be seen very clearly. In Figure 3d, the temperature distribution along $y = 0.3$ cm line from the *ISS* and the *Ideal* simulations lie almost on top of each other.

A quantitative estimate of the differences between the *ISS* and *Ideal* simulations are

Table 3: Spatial concentration gradients of the individual components in Mixture T1.

	Spatial concentration gradient		
Component	***ISS* case**	***Ideal* case**	**Error [%]**
methane	0.1722	0.38417	-55.19
n-butane	-0.1009	-0.20045	-49.65
n-dodecane	-0.07123	-0.183725	-61.23

summarized in Table 3. In this table, the spatial concentration gradient, ∇c_i, of the i^{th} component, between the lateral walls, is computed as

$$\nabla c_i = \frac{c_i^{\text{cold}} - c_i^{\text{hot}}}{L_x}, \tag{10}$$

where c_i^{cold} and c_i^{hot} are the concentration of the i^{th} component at the cold and hot wall, respectively. As seen in this table, the relative difference of the three components are approximately between 50-60%. It must be stated that the diffusion time of this mixture is about 56 hours (Srinivasan, Dejmeck, and Saghir, 2010) and these errors are calculated at approximately 18.5 hours. However, as mentioned earlier, by about 18 hours the mixture reaches a quasi steady state and there is less than 0.04% change in the concentrations between this time and the state of the mixture at $t \approx 56$ hours (Srinivasan, Dejmeck, and Saghir, 2010). Hence, keeping in mind that the noisy environment of ISS is not likely to help any further with the separation and neglecting the further 0.04% separation in the *Ideal* simulation, we can conclude that performing these experiments on the ISS can result in at least 50% under prediction of separation of the components.

3.2 n-dodecane/isobutylbenzene/tetralin mixture

In this low pressure ternary mixture, the CFD simulations predict the separation of the three components as follows: nC_{12} separates to the hot side while IBB and THN separate to the cold side. These separation trends are evident in Figures 4a-4c, where the mole fractions of the three components along $y = 0.25$ cm is shown.

As seen in this figure, a comparison of the *ISS* results (open circle symbols) with the *Ideal* simulation data (closed circle symbols) shows a profound effect of the vibration on the *Soret* separation. More precisely, the magnitude of vibrations are too strong, inducing convective flows that result in an almost complete mixing in the domain. On the other hand, the effect of the vibrations on the temperature profiles seems to be negligible with the *ISS* as well as the *Ideal* simulation data

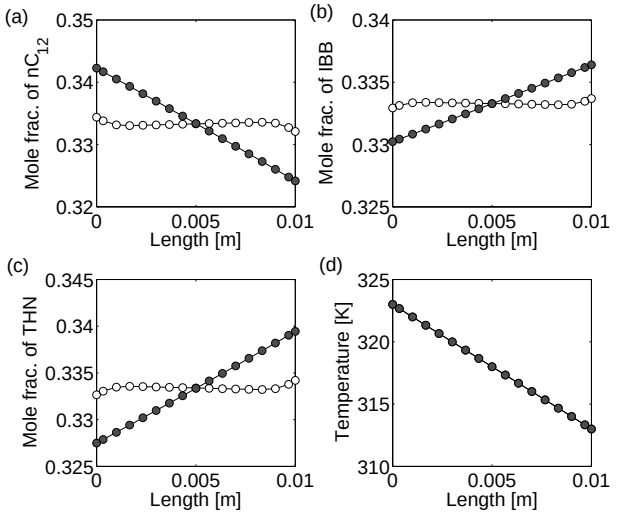

Figure 4: Distribution of (a) *n-dodecane* (b) IBB (c) THN and (d) temperature along $y = 0.25$ cm line after about 18.5 hours. Open and closed symbols represent the *ISS* and *Ideal* case, respectively.

lying on top of each other.

Velocities in the x and y directions along $y = 0.25$ cm line, and the average flow profile in the domain after about 18.5 hours are shown in Figures 5a-5c. As seen in parts (a) and (b) of this figure, in the *ISS* case, there is a dominant velocity in the y direction, with a magnitude of the order of 1×10^{-5} m/s. This is two orders of magnitude larger than the velocity in the x direction. In the ideal case, the velocity in both directions is of the order of 1×10^{-50} m/s.

Comparing the *ISS* case of these figures with the ones from the the high pressure mixture (c.f. Figures 2a-2c) we see that unlike the high pressure case, where the velocities were dominant only near the walls, there is a noticeable motion all along the domain. Also, as in mixture T1, there is a single convective flow cell established in the domain that produces a mixing effect in the domain. Overall, there seems to be a much stronger flow in the domain that hinders the *Soret* separation in the *ISS* case.

A quantitative estimate of the differences between the *ISS* and *Ideal* simulations are summarized in Table 4. In this low pressure ternary mixture, we notice an even higher error in the spatial concentration gradient of the three components, when compared to the high pressure ternary mixture. More precisely, the *ISS* simula-

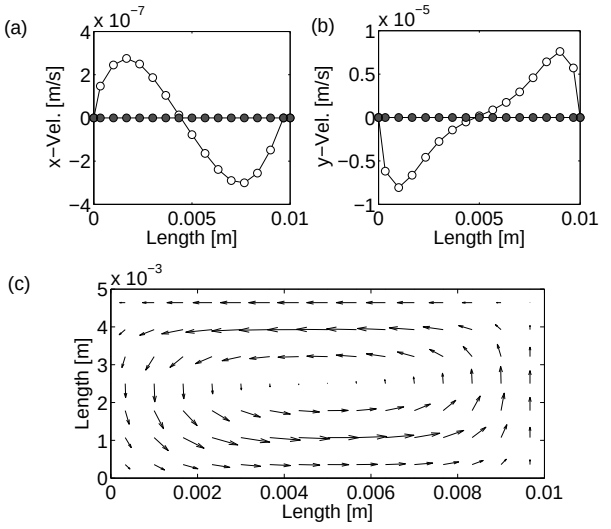

Figure 5: Velocities in the (a) x and (b) y directions along $y = 0.25$ cm line, and (c) the average flow profile in the domain after about 18.5 hours. Open and closed symbols represent the *ISS* and *Ideal* case, respectively.

Table 4: Spatial concentration gradients of the individual components in Mixture T2.

	Spatial concentration gradient		
Component	***ISS* case**	***Ideal* case**	**Error [%]**
nC_{12}	0.2303	1.8114	-87.29
IBB	-0.0758	-0.6166	-87.71
THN	-0.1544	-1.1948	-87.08

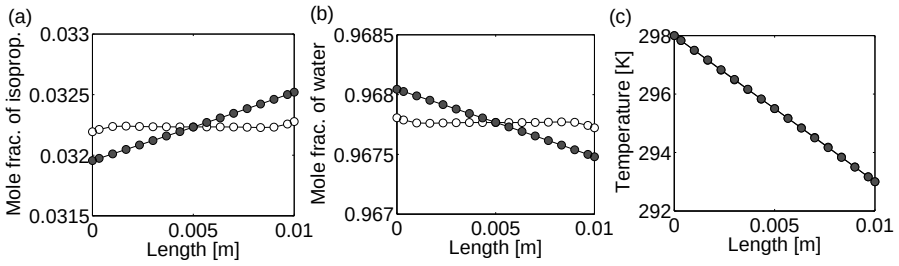

Figure 6: Distribution of (a) *isopropanol* (b) *water* and (c) temperature along $y = 0.5$ cm line after about 18.5 hours. Open and closed symbols represent the *ISS* and *Ideal* case, respectively.

tion under predicts the separation of all three components by approximately 87%. However, there is no disagreement in predicting the direction of separation of the three components. The higher error can be attributed to the fact that at a lower pressure it is relatively easier for the fluid to flow freely. In other words, for the same vibration disturbance, the response of the fluid in the form of the motion of the components is much larger when the mixture is at a lower pressure. Of course, needless to say there is also some contribution from the mixture properties, applied temperature gradient, etc. in creating this difference in the errors. Nevertheless, to validate the claim of the pressure difference being the primary factor in explaining this large jump in error of the spatial concentration gradient, a binary mixture of *isopropanol*/*water* at a pressure of 0.101325 MPa has been investigated.

3.3 Water/isopropanol mixture

In this low pressure associating mixture, due to the *Soret effect*, *isopropanol* separates towards the cold wall and water moves to the hot wall. The concentration of the two components and the temperature in the domain along $y = 0.5$ cm line at about 18.5 hours is shown in Figures 6a-6c. Once again, the open symbols represent the *ISS* case and the closed symbols represent the *Ideal* case. As in the other two mixtures, we can see in these figures that in the *ISS* case there is a much weaker separation.

As before, the disagreements between the *ISS* and the *Ideal* cases can be attributed to the ISS vibrations that impede this separation behavior by inducing a convective flow in the domain. The strong flow in the *ISS* case is evident in the form of large velocities in the two directions along $y = 0.5$ cm line at about 18.5 hours in Figures 7a and 7b. As in the previous two mixtures, the velocity in either direction

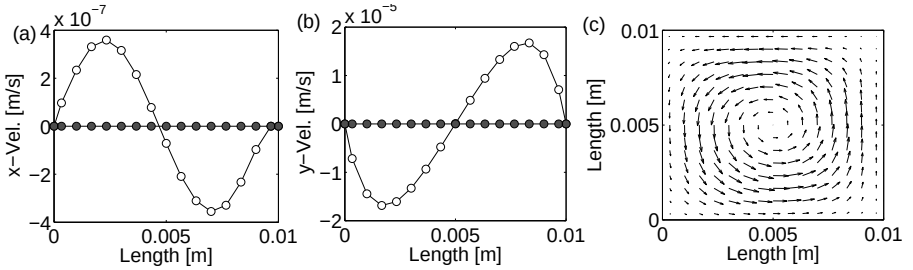

Figure 7: Velocities in the (a) x and (b) y directions along $y = 0.5$ cm line, and (c) the average flow profile in the domain after about 18.5 hours. Open and closed symbols represent the *ISS* and *Ideal* case, respectively.

Table 5: Spatial concentration gradients of the individual components in Mixture B1.

Spatial concentration gradient			
Component	***ISS* case**	***Ideal* case**	**Error [%]**
isopropanol	-0.0084	-0.0564	-85.11
water	0.0084	0.0564	-85.11

in the *Ideal* case is of the order of 1×10^{-50} m/s. In the *ISS* case, y velocity is O(1×10^{-5} m/s), two orders of magnitude larger than the x velocity. An important observation is that unlike the mixture T1 where velocities were only large near the walls, there is a strong motion all along the domain. In fact, one can see a sinusoidal velocity profile in both directions. As a consequence of such strong vibrations, a single convective cell is established in the *ISS* simulation, similar to the two ternary systems. This is seen in Figure 7c where the average flow in the last fifty seconds in the domain at the end of the simulation is shown.

The spatial concentration gradient computed from Equation (10) is summarized in Table 5. The table also includes the relative error in ∇c_i between the *ISS* and *Ideal* case. As seen in this table, in the *ISS* case there is an under prediction of the separation of the components by about 85%. Further, this error is about the same as in the low pressure ternary hydrocarbon mixture and is much higher than the high pressure ternary mixture. From the comparison of the errors between these three systems, it can be said that the lower pressure of the mixtures T2 and B1 are responsible for the higher errors. More specifically, as a result of the lower

pressure, the fluid responds more easily to applied vibrations.

4 Summary & Conclusions

Two-dimensional CFD simulations have been made to understand the impact of the vibrations on board the International Space Station on the thermodiffusion process in two ternary hydrocarbon mixtures and a binary associating mixture of *isopropanol* and *water*. While the first ternary mixture was at a pressure of 35 MPa, the other two mixtures had a mean pressure of 0.101325 MPa.

For each mixture, two simulations were made. In the first case (*Ideal*), an ideal thermodiffusion process was simulated by assuming zero gravity conditions. In the second case (*ISS*), the vibrating environment of the ISS was simulated by making use of the acceleration values recorded on the ISS. The following observations were made: (a) The ISS vibrations were too strong for all three mixtures, resulting in a single convective cell in all the systems. Further, the flow was such that there was a significant amount of mixing in the cell that minimized the *Soret* separation. (b) In all three systems, in the *ISS* simulations, the y component of the velocity was two orders of magnitude larger than the x component. Also, while in the high pressure mixture, the *ISS* case showed strong velocity components only closer to the vertical walls, in the low pressure systems there were noticeable velocity components throughout the domain. (c) A comparison of the *ISS* case with the *Ideal* case in all three mixtures showed that because of the mixing effect, the *ISS* case produces a spatial concentration gradient that is anywhere between 55% (for the high pressure mixture) and 85% (for the low pressure mixture) lower than the ones realized from the *Ideal* simulations. The larger error in the low pressure mixtures is due to the fact that at lower pressure the fluid responds easily to the applied vibrations.

In summary, it can be stated that performing diffusion investigations for liquid mixtures on the ISS is prone to non-negligible errors that arise due to the vibrations of the platform. Further, while the error decreases for fluids at high pressure, there is still a significant amount of convective disturbance that will destroy the small separations that are obtained via the *Soret effect*. Hence, it is advisable to use the vibration isolation facility that is available on the ISS to conduct pure diffusion investigations like the ones in this study.

Acknowledgement: The authors thank the Canadian Space Agency and the European Space Agency for funding this research.

References

Chacha, M.; Faruque, D.; Saghir, M. Z.; Legros, J. C. (2002): Solutal Thermodiffusion in Binary Mixture in the Presence of G-jitter. *International Journal of Thermal Sciences*, vol. 41, pp. 899–911.

Chacha, M.; Saghir, M. Z. (2005): Solutal-Thermo-Diffusion Convection in a Vibrating Rectangular Cavity. *International Journal of Thermal Sciences*, vol. 44, pp. 1–10.

Davidson, B. J. (1973): Heat Transfer from a Vibrating Circular Cylinder. *Internation Journal of Heat and Mass Transfer*, vol. 16, pp. 1703.

Gershuni, G. Z.; Kolesnikov, A. K.; Legros, J. C.; Myznikova, B. L. (1999): On the Vibrational Convective Instability of a Horizontal Binary-Mixture Layer with Soret Effect Under Transversal High Frequency Vibration. *International Journal of Heat and Mass Transfer*, vol. 42, pp. 547.

Gershuni, G. Z.; Zhukhovitsky, E. M. (1981): Convective Instability of a Fluid in a Vibrational Field Under Conditions of Weightlessness. *Fluid Dynamics*, vol. 16, pp. 498.

Ghorayeb, K.; Firoozabadi, A. (2000): Molecular, pressure, and thermal diffusion in non-ideal multicomponent mixtures. *American Institute of Chemical Engineers Journal*, vol. 46, no. 5, pp. 883–891.

Lohrenz, J.; Bray, B. G.; Clark, C. (1964): Calculating Viscosities of Reservoir Fluids from their Compositions. *Journal of Petroleum Technology*, vol. 16, no. 10, pp. 1171–1176.

Merkin, J. H. (1967): Oscillatory Free Convection from an Infinite Horizontal Cylinder. *Journal of Fluid Mechanics*, vol. 30, pp. 561.

Monti, R.; Savino, R.; Lappa, M. (2001): On the Convective Disturbances Induced by G-jitters on the Space Station. *Acta Astronautica*, vol. 48, no. 5-12, pp. 603.

NIST (2007): Thermophysical properties of hydrocarbon mixtures database. National Institute of Standards and Technology, 2007. version 3.2.

Parsa, A.; Srinivasan, S.; Saghir, M. Z. (2010): Impact of Density Gradients on the Fluid Flow Inside a Vibrating Cavity Subjected to Soret Effect. *AIAA Journal*. submitted.

Patankar, S. V. (1980): *Numerical Heat Transfer and Fluid Flow*. McGraw Hill, New York.

Savino, R.; Lappa, M. (2003): Assessment of Thermovibrational Theory: Application to G-jitter on the Space Station. *Journal of Spacecraft and Rockets*, vol. 40, no. 2, pp. 201.

Srinivasan, S.; Dejmeck, M.; Saghir, M. Z. (2010): Thermo-Solutal-Diffusion In High Pressure Liquid Mixtures In the Presence of Micro-Vibrations. *International Journal of Thermal Sciences*, vol. 49, pp. 1613–1624.

Srinivasan, S.; Eslamian, M.; Saghir, M. Z. (2009): Estimation of the Thermodiffusion Coefficients for n-Dodecane/n-Butane/Methane Mixtures and Comparison with Experimental Data from Foton M3 Mission. *IAC*, , no. IAC-09-A2.3.1.

Srinivasan, S.; Saghir, M. Z. (2009): Experimental Data on Thermodiffusion in Ternary Hydrocarbon Mixtures. *Journal of Chemical Physics*, vol. 131, pp. 124508.

Srinivasan, S.; Saghir, M. Z. (2010): Significance of Equation of State and Viscosity on the Thermodiffusion Coefficients of a Ternary Hydrocarbon Mixture. *High Temperatures High Pressures*, vol. 39, pp. 65–81.

Van Vaerenbergh, S.; Srinivasan, S.; Saghir, M. Z. (2009): Thermodiffusion in Multi-Component Hydrocarbon Mixtures: Experimental Investigations and Computational Analysis. *Journal of Chemical Physics*, vol. 131, pp. 114505.

Yan, Y.; Jules, K.; Saghir, M. Z. (2007): A Comparative Study of G-jitter Effect on Thermal Diffusion Aboard the International Spacestation. *Fluid Dynamics and Material Processing Journal*, vol. 3, no. 3, pp. 231–245.

Yan, Y.; Pan, S.; Jules, K.; Saghir, M. Z. (2007): Vibrational Effect on Thermal Diffusion Under Different Microgravity Environments. *Microgravity Science and Technology*, vol. 19, no. 2, pp. 12–25.